Oleyl Sulfate Reveals Allosteric Inhibition of Soybean Lipoxygenase-1 and Human 15-Lipoxygenase†

Rakesh Mogul, Eric Johansen, and Theodore R. Holman*

Department of Chemistry and Biochemistry, University of California, Santa Cruz, California 95064

Received December 7, 1999; Revised Manuscript Received February 9, 2000

ABSTRACT: Inhibition of lipoxygenase (LO) is currently an important goal of biomedical research due to its critical role in asthma, atherosclerosis, and cancer regulation. Steady-state kinetic data indicate that oleic acid (OA) is a simple competitive inhibitor for soybean lipoxygenase; however, kinetic isotope effect (KIE) data suggest a more complicated inhibitory mechanism. To investigate the inhibitory effects of fatty acids on lipoxygenase more thoroughly, we have synthesized a novel inhibitor to lipoxygenase, (*Z*)-9-octadecenyl sulfate (oleyl sulfate, OS), which imparts kinetic properties that are inconsistent with simple competitive inhibition for both SLO-1 and 15-HLO. The KIE exhibits a hyperbolic rise with addition of OS, indicating the formation of a catalytically active ternary complex with K_D values of 0.6 ± 0.2 and 0.4 ± 0.05 μM for SLO-1 and 15-HLO, respectively. The steady-state kinetics show that SLO-1 proceeds through a hyperbolic mixed-type inhibition pathway, where OS binding ($K_i = 0.7 \pm 0.3$ μM) causes an approximate 4-fold increase in the K_m(app) ($\alpha = 4.6 \pm 0.5$) and a decrease in the k_{cat} by approximately 15% ($\beta = 0.85 \pm 0.1$). 15-HLO also exhibits a hyperbolic saturation of k_{cat}/K_m consistent with the observed rise in its KIE. Taken together, these findings indicate the presence of an allosteric site in both SLO-1 and 15-HLO and suggest broad implications regarding the inhibition of LO and the treatment of LO-related diseases.

Inhibition of lipoxygenases (LO)[1] is an important area of investigation due to their involvement in a number of inflammatory diseases (*1*, *2*) and cancer growth regulation (*3*−*5*). They are present in a wide variety of organisms and catalyze the oxidation of unsaturated fatty acids utilizing an essential, non-heme iron atom (*6*). The generally accepted mechanism for lipoxygenases involves a hydrogen atom abstraction at C-3 of the 1,4-diene by Fe(III), with subsequent trapping of the pentadienyl radical by oxygen, forming the hydroperoxide product (*7*−*9*). Soybean lipoxygenase (SLO-1) manifests an extremely large kinetic isotope effect (KIE $= {}^{D}[k_{cat}/K_m] \approx 80$), where the rate-determining step (RDS), below 32 °C, is limited by diffusion, solvent isotopes, and C−H abstraction (*10*−*12*). Above 32 °C, the RDS is fully limited by C−H abstraction, as seen by the temperature-independent behavior of the KIE. Recently, we have shown that 15-human lipoxygenase (15-HLO) also exhibits a large KIE (≈60) at 5 μM linoleic acid (LA) and that it manifests a temperature dependence similar to that of SLO-1 (*13*). At 100 μM LA (5 °C), however, the KIE increases dramatically and is completely temperature independent, for both 15-HLO and SLO-1 (*13*). This suggests that at 100 μM LA, C−H abstraction is fully rate-limiting from 5 to 35 °C for both 15-HLO and SLO-1. The KIE of SLO-1 and 15-HLO is also elevated and temperature independent upon addition of oleic acid (OA), indicating that both LA and OA change the microscopic kinetic rate constants (*13*). This change in the microscopic rate constants is postulated to be due to the presence of an allosteric site (*13*), as previously suggested for SLO-1 and human 5-lipoxygenase (*14*, *15*). The interpretation of the increased KIE, however, is complicated by the fact that LA and OA have low solubilities which can affect their solution state structures (i.e., monomer substrate versus aggregated substrate). To address this issue, we have synthesized a novel inhibitor to lipoxygenase, (*Z*)-9-octadecenyl sulfate (oleyl sulfate, OS), which is over 3 times more soluble than OA and imparts kinetic properties that are inconsistent with simple competitive inhibition. These results strongly suggest the presence of an allosteric site that modulates catalysis by lowering the specificity constant (k_{cat}/K_m) by ≈80% for both SLO-1 and 15-HLO.

MATERIALS AND METHODS

Materials. SLO-1 and 15-HLO were expressed and purified as described previously (*16*). Iron contents of SLO-1 and 15-HLO were determined on a Finnegan inductively coupled plasma mass spectrometer (ICP-MS), using standardized iron solutions. All kinetic measurements were standardized to iron content.

Fatty Acid Synthesis. OS ($C_{18}H_{36}O_4S$) and linoleyl sulfate (LS) ($C_{18}H_{34}O_4S$) were prepared by a similar procedure to that of Axelrod and co-workers (*17*). One gram of the fatty

† This work was supported by NIH Grant GM56062-01.

* To whom correspondence should be addressed. Phone: 831-459-5884. Fax: 831-459-2935. Email: tholman@chemistry.ucsc.edu.

[1] Abbreviations: SLO-1, soybean lipoxygenase-1; 15-HLO, 15-human lipoxygenase; LA, linoleic acid; OA, oleic acid; FA, fatty acid; OS, oleyl sulfate or (*Z*)-9-octadecenyl sulfate; LS, linoleyl sulfate; SDS, sodium lauryl sulfate; D-LA, perdeuterated LA; 13-HPOD, 13-hydroperoxy-9,11-(*Z*,*E*)-octadecadienoic acid; RP-HPLC, reverse phase HPLC; RDS, rate-determining step; EI-MS, electron ionization mass spectroscopy; ICP-MS, inductively coupled plasma mass spectroscopy; TLC, thin-layer chromotography; NMR, nuclear magnetic resonance; CMC, critical micelle concentration.

10.1021/bi992805t CCC: $19.00
Published on Web 03/31/2000

acid was dissolved under nitrogen in 3.6 mL of 1 M $LiAlH_4$ (dry THF). The mixture was refluxed for 2 h and quenched with saturated NH_4Cl. The solution was filtered, dried over Na_2SO_4, and evaporated to dryness. The resulting oil was dissolved in 6 mL of dry pyridine, and 0.5 g of sulfamic acid was added. The reaction was heated at 95 °C for 1.5 h under nitrogen and stopped with the addition of 20 mL of methanol and 1 mL of saturated Na_2CO_3. The waste solids were filtered off, and the solution was evaporated to dryness. The resulting residue was recrystallized from hot methanol, and the white solid gave a single spot by TLC (silica gel), developed in hexane/ether/acetic acid (60:39:1). The ^1H NMR signals ($CDCl_3$) for OS were observed at δ 5.35 (br m, 2H), 4.02 (t, 2H), 2.01 (br m, 4H), 1.65 (br m, 2H), 1.30 (br m, 22H), 0.89 (t, 3H). The ^1H NMR signals ($CDCl_3$) for LS were observed at δ 5.35 (br m, 4H), 4.02 (t, 2H), 2.77 (t, 2H), 2.05 (q, 4H), 1.66 (br m, 2H), 1.33 (br m, 16H), 0.90 (t, 3H).

Fatty Acid Purification. LA was purchased from Aldrich Chemical Co., and perdeuterated linoleic acid (D-LA) was purified from a mixture of perdeuterated algal fatty acids from Cambridge Isotope labs. The algal fatty acid mixture was esterified, loaded onto a 10% Ag−silica column (800 g of silica), washed with hexane, and eluted with ethyl acetate/hexane (2:98). The fractions were analyzed by electron ionization mass spectroscopy (EI-MS), and those containing D-LA were combined, evaporated to dryness, and de-esterified overnight, with an ethanol/2.5 M NaOH (aqueous) mixture (50:50). The sample was then extracted with CH_2Cl_2 and evaporated to dryness. The D-LA was depleted of monoprotonated substrate with SLO-1, exhaustively extracted with CH_2Cl_2, and purified twice by a Waters 625 HPLC with a C18 column (Higgins Analytical, 5 μm, 250 × 10 mm, isocratic mobile phase: 86.9% methanol/13% H_2O/0.1% acetic acid at 3 mL/min). Substrate was detected by on-line UV absorption (210 nm) and had a retention time of approximately 30 min. Substrate fractions were collected, evaporated to dryness, redissolved in ethanol, and stored at −20 °C. The LA was also purified by RP-HPLC and combined with D-LA to the appropriate ratio. The LA:D-LA ratio was verified by complete conversion to the products with SLO-1, and the LA and D-LA products were separated by HPLC (vide infra). A negative control is performed to ensure that autoxidized substrate is not present in the substrate mixture. This is critical because impurities can dramatically affect the KIE values. The concentration of substrate was determined by enzymatically converting 1 mL of diluted LA stock to product. The product absorbs at 234 nm with an extinction coefficient of 25 000 M^{-1} cm^{-1}. All other reagents were of analytical grade or higher.

OS Quantitation. OS was solubilized directly in water and its concentration determined by EI-MS and NMR using an internal standard of LS. LS concentrations were determined by using soybean lipoxygenase-1 to convert 100% of the LS to the hydroperoxide product (ϵ = 25 000 M^{-1} cm^{-1}, assuming a similar ϵ to 13-HPOD). Aqueous OS solutions containing fixed amounts of LS were injected via syringe pump with a continuous flow at 0.01 mL/min. Mass spectral data were obtained when the *m*/*z* signal of both compounds had stabilized and after voltage was optimized. Intensities of both compounds were averaged over several scans and concentrations determined using relative ratios. A NMR spectrum ($CDCl_3$) was taken of a similar mixture of OS and LS, and their relative ratios were determined by comparing their signal integrations. Both methods were in agreement within 15%. It should be noted that OS tends to stick to various materials which lowers its apparent concentration and care should be taken when aliquoting solutions.

Surface Tension Measurements. Buffers were used which correspond to those of the kinetic measurements. Surface tension was measured as described by Harkins et al., using a thin platinum plate (perimeter 2.5 cm) and a Cahn electromicrobalance (*18*). Various amounts of surface-active agent were added to a 30 mL buffer solution, and the surface tension was continuously recorded. After each addition, a sufficiently long period of time (≈10−30 min) was allowed to elapse before attaining a steady value of the surface tension. Critical micelle concentration (CMC) values were obtained by plotting the measured surface tensions versus the logarithm of the concentrations of the surface-active agent and recording the intercept of the two straight lines. The point at which a deviation from the straight line occurs, as observed in the surface tension versus log [surface-active agent] plot, was defined as the start of premicellular aggregate formation (*18, 19*).

Kinetic Isotope Effect Determination. Determination of the kinetic isotope effect (KIE) was similar to that previously published by Holman and co-workers with the following modifications (*13*). Lipoxygenase is added (≈0.12 nM SLO-1 and ≈12 nM 15-HLO) to a protio/perdeutero LA mixture (60 mL, 5 μM LA/D-LA), monitored at 234 nm with a P-E Lambda 4 and stopped with an acid quench (≈5% glacial acetic acid) at less than 5% total LA/D-LA consumption. It is important to note that diode array spectrophotometers degrade 13-hydroperoxy-9,11-(*Z*,*E*)-octadecadienoic acid (13-HPOD) and care should be taken if the reaction time length is longer than 5 min. The acidified reaction mixture is extracted with methylene chloride (trimethyl phosphite, which quantitatively reduces the labile 13-HPOD, is not needed since both the alcohol and the peroxide have the same elution time). The methylene chloride layer is evaporated to dryness under vacuum, reconstituted in 50 μL of running buffer, injected onto a C18 column (Higgins Analytical, 5 μm, 250 × 4.6 mm), and eluted at 1 mL/min (isocratic mobile phase: 74.9% methanol/25% H_2O/0.1% acetic acid). As described previously by our lab, RP-HPLC separates the perdeutero 13-HPOD from the protio 13-HPOD with base line separation and retention times of approximately 20 and 22 min, respectively (*13*). The molar protio/perdeutero 13-HPOD ratios are equated to the corresponding peak area ratios, and the competitive KIE ($^D[k_{cat}/K_m]$) is then calculated from: $\ln (1 - f)/[\ln (1 - (fR_P/R_O))]$, where R_O is the mass ratio of the starting substrate and R_P is the mass ratio of the product at the extent of reaction *f*. When the percent conversion (*f*) to product is less than 5%, this equation simplifies to: $([P-H]/[P-D])([S_o-D]/[S_o-H])$, where [P−H] is protio−product concentration and $[S_o-H]$ is the initial protio−substrate concentration (*20*). Both equations gave comparable results within experimental error. The typical ratio of perdeutero to protio substrate is approximately 2:1, respectively. Greater substrate ratios than 2:1 were not used due to the expensive nature of the perdeutero substrate. Under these conditions, the upper limit for the KIE is greater than 130 and is limited by the vanishingly small peak area of the

perdeutero 13-HPOD peak relative to the negative control. This RP-HPLC-based method for determining molar protio/perdeutero 13-HPOD ratios gave results identical (within experimental error) to those obtained by EI-MS. We see no appreciable side products at any wavelength for 15-HLO or SLO-1, indicating no reaction branching. The OS titration experiments require 5 μM LA/D-LA to record product ratios. For the 15-HLO experiments (pH 7.5), OS concentrations above 6 μM were not feasible due to large amounts of a white emulsion at the extraction interface which inhibited product recovery. This emulsion was not observed for reactions performed with SLO-1 (pH 9.2). We believe that the emulsion may be due to a precipitated protein/fatty acid aggregate because the 15-HLO reaction has over 100-fold more enzyme and not due to a pH difference since both extractions contain excess acetic acid. All kinetic data reported were measured in triplicate on two distinct days.

Steady-State Kinetics. Lipoxygenase rates were determined by following the formation of product at 234 nm ($\epsilon = 25\,000$ M^{-1} cm^{-1}) with a Hewlett-Packard 8453 UV−vis spectrophotometer. The destruction of 13-HPOD by the diode array spectrophotometer was negligible under these reaction conditions. All reactions were 2 mL in volume, run at room temperature (23 °C), and constantly stirred with a rotating magnetic bar. In experiments using SLO-1, kinetic reactions were performed in 0.1 M borate (pH 9.2), while reactions using 15-HLO were performed in 25 mM HEPES (pH 7.5). Substrate solutions used in each experiment were measured for accurate LA concentration by quantitatively converting substrate to product using soybean lipoxygenase-1. Enzymatic rates were measured between 1 and 50 μM LA with 1−25 μM OS for SLO-1 and lower than 2 μM LA for 15-HLO. Solutions containing LA and/or OS were sonicated for 3−5 min before use in kinetic experiments. Rate reactions were initiated by the addition of enzyme to final concentrations of ≈3 nM SLO-1 (≈80% iron content) and ≈200 nM 15-HLO (≈15% iron content). All kinetic parameters were determined by nonlinear regression using Kaleidagraph software (Abelbeck).

Viscosity. Buffer and substrate solutions of 0 and 30 % (w/v) glucose, in 0.1 M CHES buffer, pH 9.2, 20 °C, were prepared corresponding to relative viscosities (η_{rel}) of 1 and 3, respectively ($\eta_{rel} = \eta/\eta^o$, η^o is the viscosity of H_2O at 20 °C, *CRC Handbook of Chemistry*). Sucrose and ethylene glycol were not used as viscogenic agents due to inhibition, and borate reacts with glucose to lower its buffering capacity (*11*).

RESULTS

Surface Tension Measurements. CMC values have been determined for LA in 0.1 M borate (pH 9.2) and 25 mM HEPES (pH 7.5) to be 150 ± 10 and 40 ± 10 μM, respectively (data not shown). These values correlate well with those of the literature and indicate the dramatic loss in solubility of LA as pH decreases (*19*). Addition of 16 μM OS has no significant effect on the CMC of LA at pH 9.2. However, at pH 7.5, addition of 5 and 10 μM OS results in a deviation from linear behavior at approximately 25 ± 5 μM total fatty acid (FA) concentration (LA and OS). This indicates the formation of mixed premicellular aggregates of LA and OS, possibly due to hydrogen bond interactions between the protonated LA and the deprotonated OS (*21*). These aggregates could conceivably be enzymatic substrates, and for this reason, only kinetic data below 20 μM total FA (pH 7.5) are used in the current study for 15-HLO.

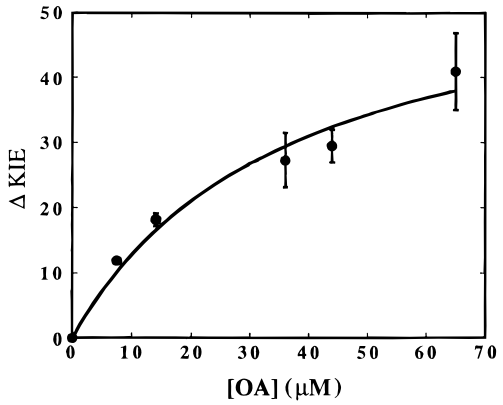

FIGURE 1: Effect of [OA] on the change in KIE (Δ KIE) for SLO-1 (pH 9.2, 100 mM borate, 5 °C, and 5 μM H/D substrate mixture). The hyperbolic fit yields a K_D of 36 ± 14 μM ($R^2 = 0.98$, RMS = 2.1), where the initial KIE is 15.

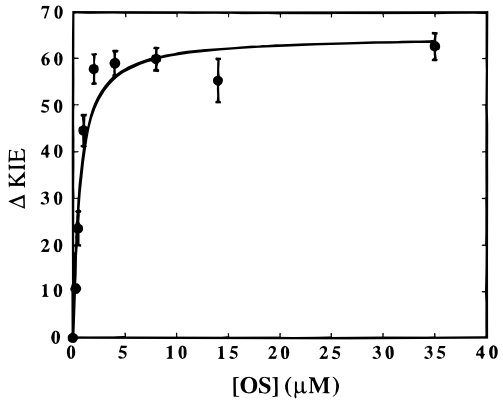

FIGURE 2: Effect of [OS] on the change in KIE (Δ KIE) for SLO-1 (pH 9.2, 100 mM borate, 5 °C, and 5 μM H/D substrate mixture). The hyperbolic fit yields a K_D of 0.6 ± 0.2 μM ($R^2 = 0.94$, RMS = 5.1), where the initial KIE is 15.

Kinetic Isotope Effect. Previously, we have shown that OA increases the KIE of SLO-1 (*13*). Titration of increasing amounts of OA, into a constant LA/D-LA mixture of 5 μM, reveals a hyperbolic rise in the KIE which suggests the formation of a catalytically active ternary complex. The data can be fit to a simple saturation curve yielding a K_D of 36 ± 14 μM OA (Figure 1) (*13*). This value is within experimental error of the accepted K_i for OA ($K_i \approx 22$ μM)(*22*), which supports a direct correlation between OA inhibition and the rise in KIE. To investigate this effect further, we have performed a series of KIE experiments for both SLO-1 and 15-HLO with OS, a more soluble analogue of OA, that has never before been used as a lipoxygenase inhibitor. As shown in Figure 2, the KIE of SLO-1 sharply rises as OS is added. A hyperbolic fit to the change in KIE (Δ KIE) yields a K_D value of 0.6 ± 0.2 μM, which represents an approximate 60-fold increase in binding affinity over that of OA. The KIE for 15-HLO also manifests a hyperbolic increase as OS is added, yielding a K_D value of 0.4 ± 0.05 μM (Figure 3). The increase in KIE for both SLO-1 and 15-HLO can best be explained by a decrease in commitment (k_2/k_{-1}). The kinetic mechanism for SLO-1 can be minimally described by Scheme 1, where k_2 is the RDS and k_{-2} is ≈0 (k_2 is

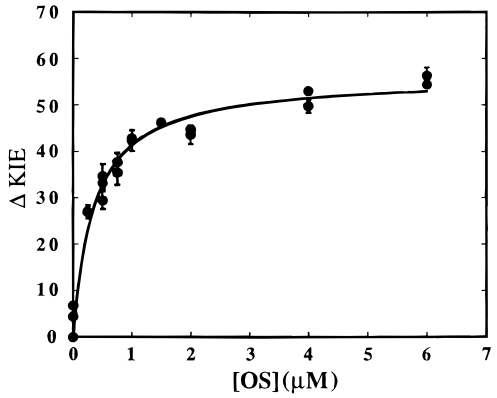

FIGURE 3: Effect of [OS] on the change in KIE (Δ KIE) for 15-HLO (pH 7.5, 25 mM HEPES, 5 °C, and 5 μM H/D substrate mixture). The hyperbolic fit yields a K_D of 0.4 ± 0.05 μM (R^2 = 0.96, RMS = 2.9), where the initial KIE is 18.

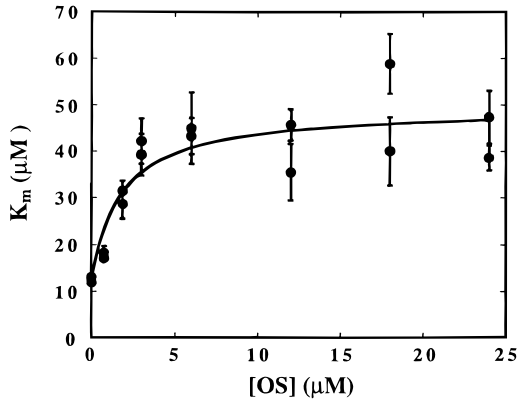

FIGURE 4: Effect of [OS] on K_m(app) for SLO-1 (pH 9.2, 100 mM borate, 25 °C, and 1−50 μM LA, for each inhibitor point). The line is a fit to the experimental points with eq 3 (Scheme 2), where K_m = 12.4 μM. α and K_i were determined to be 4 ± 0.3 and 0.45 ± 0.16 μM, respectively (R^2 = 0.83, RMS = 5.6).

Scheme 1

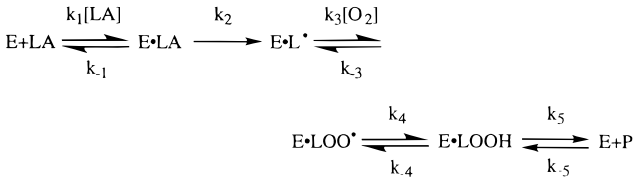

approximately 5000-fold greater than k_{-2}). This was previously determined by Klinman and co-workers and is considered an accurate description of the SLO-1 reaction for this study (*9*). According to Scheme 1, the KIE is described by the following equation:

$$\mathrm{KIE} = {}^{D}[k_{cat}/K_m] = (k_{cat}/K_m)^{H}/(k_{cat}/K_m)^{D} = (k_2{}^{H}/k_2{}^{D} + k_2{}^{H}/k_{-1}{}^{H})/(1 + k_2{}^{H}/k_{-1}{}^{H}) \quad (1)$$

where substrate release (k_{-1}) and C−H bond cleavage (k_2) are the primary determinants for the KIE (this assumes k_2 = k_{cat}). The KIE increases to a maximum of $k_2{}^{H}/k_2{}^{D}$ when commitment ($k_2{}^{H}/k_{-1}{}^{H}$) is small and decreases, approaching 1, when commitment is large. This assumes that the intrinsic $k_2{}^{H}/k_2{}^{D}$ remains unchanged. Control experiments using SDS revealed no increase in the KIE and thus eliminate the possibility of nonspecific surfactant binding as a cause for the increase in KIE.

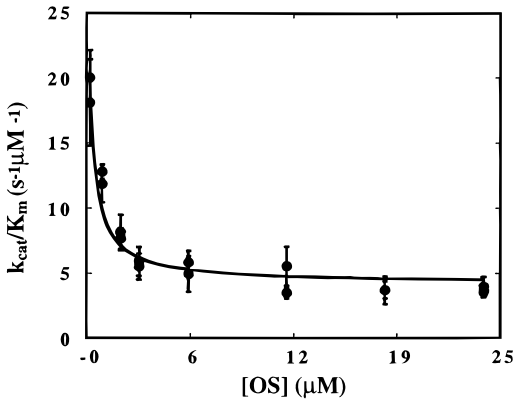

FIGURE 5: Effect of [OS] on k_{cat}/K_m for SLO-1 (pH 9.2, 100 mM borate, 25 °C, and 1−50 μM LA, for each inhibitor point). The line is a fit to the experimental points with eq 4 (Scheme 2), where K_m = 12.4 μM, k_{cat} = 237 s^{-1}, α = 4, and K_i = 0.45 μM. β was determined to be 0.9 ± 0.1 (R^2 = 0.95, RMS = 1.2). If β is estimated to be 0.85 (from Figure 6), then the fit reveals α to be 5.2 ± 0.6 and K_i to be 0.86 ± 0.11 (R^2 = 0.98, RMS = 0.72) (fit not shown). The average values for α and K_i, from both the K_m-(app) and k_{cat}/K_m fits, are 4.6 ± 0.5 and 0.7 ± 0.3 μM, respectively.

Inhibition Studies. The steady-state kinetic parameters were determined for both SLO-1 and 15-HLO with increasing amounts of OS. SLO-1 exhibits a striking hyperbolic response to increasing amounts of OS with an increase in K_m(app) from 12.5 μM to a saturating value of ≈50 μM (Figure 4). The k_{cat}/K_m (s^{-1} μM^{-1}) decreases from 19 to ≈5 s^{-1} μM^{-1} (Figure 5), while k_{cat} decreases from 237 to ≈180 s^{-1} (Figure 6). The saturation behavior of K_m(app) and k_{cat}/K_m is indicative of hyperbolic inhibition (i.e., partial inhibition), which suggests the presence of an allosteric binding site that affects catalysis by changing the microscopic rate constants of the enzyme, Scheme 2 (*23*):

$$1/v = (\alpha K_m/k_{cat})*[([I] + K_i)/(\beta[I] + \alpha K_i)]*1/[S] + 1/k_{cat}*[([I] + \alpha K_i)/(\beta[I] + \alpha K_i)] \quad (2)$$

$$K_m(\mathrm{app}) = (\alpha K_m)*[([I] + K_i)/([I] + \alpha K_i)] \quad (3)$$

$$k_{cat}/K_m = (k_{cat}/\alpha K_m)*[(\beta[I] + \alpha K_i)/([I] + K_i)] \quad (4)$$

$$k_{cat} = k_{cat}*[(\beta[I] + \alpha K_i)/([I] + \alpha K_i)] \quad (5)$$

From Scheme 2, eqs 2−5 are derived which allow for the determination of three parameters: the strength of inhibitor binding (K_i), the change in K_m (α), and the change in k_{cat} (β). A fit to the K_m(app) saturation curve with eq 3 (k_{cat} = 237 s^{-1}, K_m = 12.4 μM) yields an α of 4.0 ± 0.3 and a K_i of 0.45 ± 0.16 μM, indicating an increase in K_m(app) by a factor of 4 (Figure 4). These values of α and K_i can be entered into eq 4 and fit to the k_{cat}/K_m data (Figure 5), which results in a β of 0.9 ± 0.1. A more precise method of determining β is from the k_{cat} data; however, the data are not accurate enough to fit directly. This is possibly due to the extended lag phase induced by high concentration of OS which could hinder an accurate determination of k_{cat}. Mathematical simulations were therefore used to determine

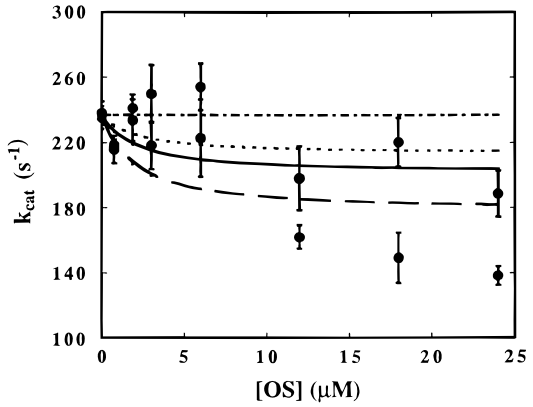

FIGURE 6: Effect of [OS] on k_{cat} for SLO-1 (pH 9.2, 100 mM borate, 25 °C, and 1−50 μM LA, for each inhibitor point). The lines are simulations to the experimental points with eq 5 (Scheme 2), where $K_m = 12.4$ μM, $k_{cat} = 237$ s^{-1}, $\alpha = 4$, $K_i = 0.45$ μM, and β is varied: (A) (− · −), $\beta = 1$; (B) (---), $\beta = 0.9$; (C) (—), $\beta = 0.85$; (D) (——), $\beta = 0.75$.

Scheme 2

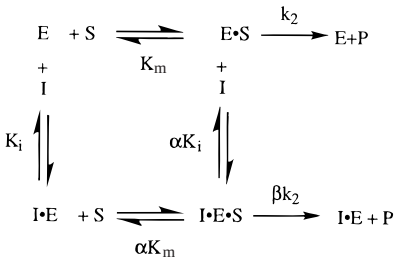

Scheme 3

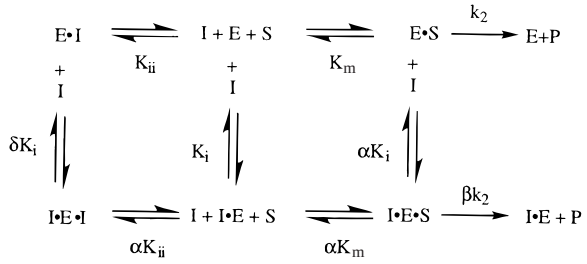

an approximate value for β (Figure 6). If the following kinetic values are entered into eq 5 ($k_{cat} = 237$ s^{-1}, $K_m = 12.4$ μM, $\alpha = 4.0$, and $K_i = 0.45$ μM) and the value for β is varied ($\beta = 0$, 0.9, 0.85, 0.75), an approximate maximal and minimal value for β can be determined. The mathematical simulations indicate that β is less than 0.9 but greater than 0.75. If we approximate β to be 0.85, according to the best fit to the k_{cat} data, and repeat the fit to the k_{cat}/K_m data (eq 4), this yields values for α and K_i of 5.2 ± 0.6 and 0.86 ± 0.11, respectively. The average values for α and K_i, derived from the K_m(app) and k_{cat}/K_m data, are 4.6 ± 0.5 and 0.7 ± 0.3, respectively, and β is approximated to be 0.85 ± 0.1. These values define the kinetics as mixed hyperbolic inhibition ($\alpha > 1$ and $\beta < 1$), yet it is clear that the major kinetic change is in the value of K_m ($\alpha = 4.6 \pm 0.5$), with only a slight shift in k_{cat} ($\beta = 0.85 \pm 0.1$). The hyperbolic inhibition data thus indicate the formation of a catalytically active ternary complex, (inhibitor−enzyme−substrate, I•E•S) and strongly suggest the presence of an allosteric site in SLO-1.

The data can also be modeled with OS binding to both the allosteric and catalytic sites (Scheme 3, eqs 6−9);

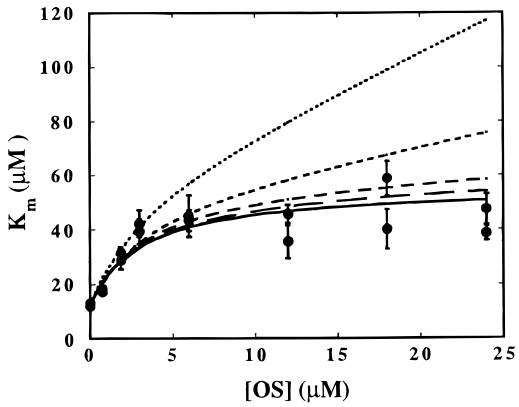

FIGURE 7: Effect of [OS] on K_m for SLO-1 (pH 9.2, 100 mM borate, 25 °C, and 1−50 μM LA, for each inhibitor point). The lines are simulations to the experimental points with eq 7 (Scheme 3), where $K_m = 12.4$ μM, $\alpha = 4.6$, $K_i = 0.7$ μM, and $\beta = 0.85$, while K_{ii} and δ are varied: (A) (—) $K_{ii} > 1000$ μM, $\delta = 1$, $R^2 = 0.78$, RMS = 6.2; (B) (— —) $K_{ii} = 100$ μM, $\delta = 4$, $R^2 = 0.72$, RMS = 7.0; (C) (— — —) $K_{ii} = 20$ μM, $\delta = 10$, $R^2 = 0.59$, RMS = 8.4; (D) (---) $K_{ii} = 50$ μM, $\delta = 1$, RMS = 15.3; (E) (···) $K_{ii} = 5$ μM, $\delta = 4$, RMS = 34.9.

however, the fit to the K_m data with eq 7 yields negative values for δ and K_{ii}, which indicate a poor model.

$$1/v = K_m/k_{cat}*[1 + [I](1/K_i + 1/K_{ii}) + [I]^2(1/\delta K_i K_{ii})]/[1 + [I](\beta/\alpha K_i)]*1/S + 1/k_{cat}*[1 + [I](1/\alpha K_i)]/[1 + [I](\beta/\alpha K_i)] \quad (6)$$

$$K_m(\text{app}) = K_m*[1 + [I](1/K_i + 1/K_{ii}) + [I]^2(1/\delta K_i K_{ii})]/[1 + [I](1/\alpha K_i)] \quad (7)$$

$$k_{cat}/K_m = k_{cat}/K_m*[1 + [I](\beta/\alpha K_i)]/[1 + [I](1/K_i + 1/K_{ii}) + [I]^2(1/\delta K_i K_{ii})] \quad (8)$$

$$k_{cat} = k_{cat}*[1 + [I](\beta/\alpha K_i)]/[1 + [I](1/\alpha K_i)] \quad (9)$$

If we attempt to mathematically simulate the K_m(app) and k_{cat}/K_m data with eqs 7 and 8, respectively ($k_{cat} = 237$ s^{-1}, $K_m = 12.4$ μM, $\alpha = 4.6$, and $K_i = 0.7$ μM) and vary δ and K_{ii}, we observe poor correlation with the data. The best simulation of the data requires a minimal value of K_{ii} to be over 140-fold (100 μM) higher than that of OS for the allosteric site and a δ of 4, comparable to α (Figures 7 and 8). The data can also be fit if the value of K_{ii} is lowered; however, the δ value increases to an unreasonably high value ($K_{ii} = 20$ μM, $\delta = 10$) (Figure 7). Therefore, these simulations demonstrate that OS weakly binds to the catalytic site and does not appreciably affect the kinetic rates. This is qualitatively demonstrated by the lack of a large increase in K_m(app) at high OS concentration. The k_{cat}/K_m data can also be simulated to Scheme 3; however, it is relatively insensitive to δ and K_{ii}, as seen by the lack of variation of the simulation curves (Figure 8). The k_{cat} data were not simulated because eq 9 does not include δ or K_{ii} terms. The substrate was not modeled as binding to the allosteric site since we do not observe appreciable substrate inhibition below 30 μM LA, as demonstrated in previous studies (*14*).

OS also induces a decrease in the k_{cat}/K_m for 15-HLO; however, due to premicellular aggregation of LA and OS at pH 7.5, only data below 20 μM total FA could be used for

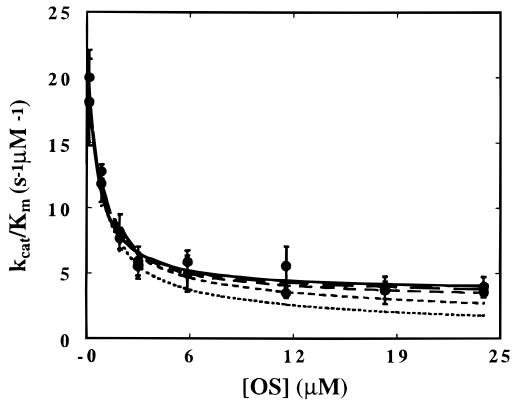

FIGURE 8: Effect of [OS] on k_{cat}/K_m for SLO-1 (pH 9.2, 100 mM borate, 25 °C, and 1−50 μM LA, for each inhibitor point). The lines are simulations to the experimental points with eq 8 (Scheme 3), where $K_m = 12.4$ μM, $k_{cat} = 237$ s^{-1}, $\alpha = 4.6$, $K_i = 0.7$ μM, and $\beta = 0.85$, while δ and K_{ii} are varied: (A) (—) $K_{ii} > 1000$ μM, $\delta = 1$, $R^2 = 0.98$, RMS = 0.79; (B) (— —) $K_{ii} = 100$ μM, $\delta = 4$, $R^2 = 0.98$, RMS = 0.78; (C) (— — —) $K_{ii} = 20$ μM, $\delta = 10$, $R^2 = 0.97$, RMS = 0.83; (D) (---) $K_{ii} = 50$ μM, $\delta = 1$, $R^2 = 0.96$, RMS = 0.99; (E) (•••) $K_{ii} = 5$ μM, $\delta = 4$, $R^2 = 0.89$, RMS = 1.66.

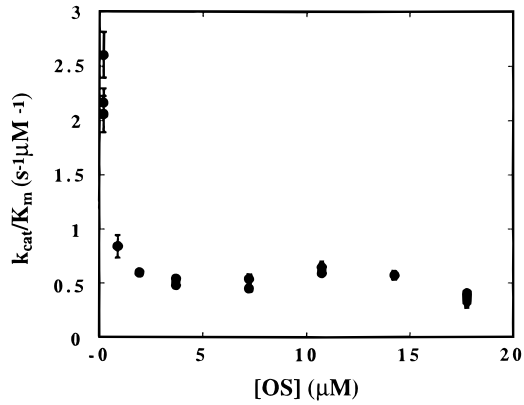

FIGURE 9: Effect of OS on K_m/k_{cat} for 15-HLO (pH 7.5, 25 mM HEPES, 25 °C), determined from initial velocities where [LA] ≪ K_m (less than 2 μM).

analysis. This reduces the available range of LA and OS concentrations and introduces a high degree of error in the mathematical fits, thus limiting any use of the steady-state K_m(app) and k_{cat} values. Consequently, we have utilized the k_{cat}/K_m values derived from the initial slope of the velocity curves, where substrate concentration is low ([LA] ≪ K_m), and we observe that k_{cat}/K_m manifests a hyperbolic decrease which cannot be explained by simple competitive inhibition (Figure 9). The decrease in k_{cat}/K_m saturates at ≈16 μM OS and is similar to the saturation behavior of its KIE. Unfortunately, α and β cannot be determined with only the k_{cat}/K_m data; however, the response of k_{cat}/K_m to addition of OS is consistent with hyperbolic inhibition.

Viscosity Measurements. Lipoxygenase is a fast enzyme that is 50% diffusion-limited ($k_{cat}/K_m \approx 3 \times 10^7$ M^{-1} s^{-1} at 20 °C) (*11*). Viscosity dependence experiments were performed on SLO-1 at 10 μM OS ($\eta/\eta^o = 1$ and 3) and clearly indicate that addition of OS abolishes all effect of viscosity on the specific activity. The $(k_{cat}/K_m^o)/(k_{cat}/K_m)$ is 1.4 ± 0.1 with no OS present and 1.0 ± 0.1 with 10 μM OS, where k_{cat}/K_m^o has an η/η^o of 1 and k_{cat}/K_m has an η/η^o of 3. This result can be explained by a decrease in commitment upon addition of OS. If we assume lipoxygenase proceeds through the previously determined reaction sequence (*9*) (i.e., Scheme 1, k_2 is the RDS and $k_{-2} \approx 0$), then the kinetic equations may be simplified and defined as

$$k_{cat}/K_m = [k_1^o(k_2/k_{-1}^o)*(\eta^o/\eta)]/[(k_2/k_{-1}^o) + (\eta^o/\eta)] \quad (10)$$

where the relative viscosity ($\eta_{rel} = \eta/\eta^o$) is the viscosity of the solution compared to aqueous solution at 20 °C and commitment is defined as k_2/k_{-1} (*9*, *11*). This equation dictates that as commitment decreases in magnitude, the effect of viscosity on k_{cat}/K_m also decreases to a limit of $[k_{cat}/K_m^o\ (\eta/\eta^o = 1)]/[k_{cat}/K_m\ (\eta/\eta^o = 3] = 1$. This limit is achieved after addition of 10 μM OS and indicates that OS binding decreases commitment for SLO-1. This treatment is general and based solely on two assumptions: (1) each microscopic bimolecular association and dissociation is diffusion-controlled, and (2) the rate of a microscopic diffusion-controlled step is inversely proportional to the viscosity of the medium as dictated by the Stokes−Einstein equation (*11*, *24*).

DISCUSSION

Previously, inhibition of SLO-1 by OA was thought to proceed through a purely competitive pathway where inhibitor and substrate compete for binding to the catalytic site (*22*). Recent studies in our lab and others, however, suggest a more complicated mechanism of inhibition for SLO-1 (*13*, *14*). In particular, we have reported a significant rise in the magnitude of the KIE with addition of OA, for both SLO-1 (Figure 1) and 15-HLO, which is inconsistent with a simple competitive inhibition model (*13*). These findings suggest the formation of a ternary complex between enzyme, substrate, and inhibitor such that commitment is lowered, thus giving rise to the increase in KIE (eq 1). Such complexes can be formed either by the presence of a regulatory site on the enzyme or through the formation of an enzymatically active LA/OA aggregate (due to the low solubility of the fatty acids) (*10*, *13*, *17*). To differentiate between these two models, a novel lipoxygenase inhibitor, OS, has been assayed revealing a dramatic increase in the KIE for both SLO-1 and 15-HLO (Figures 2 and 3). Micromolar amounts of OS impart a hyperbolic increase in the KIE (K_D values of 0.6 ± 0.2 and 0.4 ± 0.05 μM for SLO-1 and 15-HLO, respectively), which indicates a decrease in commitment (k_2^H/k_{-1}^H), as defined by eq 1. The formation of fatty acid aggregates cannot explain the higher KIE values since the LA/OS mixture concentration is well below the OS aggregation point, as shown by surface tension measurements. This increase in KIE strongly suggests the formation of a catalytically active ternary complex (substrate−enzyme−inhibitor) through OS binding to an allosteric site.

The steady-state inhibition kinetics of SLO-1 support this conclusion with an observed hyperbolic increase in K_m(app) and decrease in k_{cat}/K_m. These data cannot be described by simple competitive inhibition kinetics but rather require a hyperbolic inhibition model with an allosteric binding site (Scheme 2). The K_m(app) saturates at ≈50 μM ($\alpha = 4.6 \pm 0.5$), while the k_{cat} decreases to ≈180 s^{-1} ($\beta = 0.85 \pm 0.1$), which are indicative of a large increase in the substrate off-rate (k_{-1}) and a slight decrease in k_2 [i.e., a decrease in

commitment (k_2^H/k_{-1}^H)]. The decrease in commitment is independently corroborated by the loss of the viscosity dependence of SLO-1 with addition of OS. This loss of viscosity dependence due to the addition of OS clearly shows that commitment (k_2/k_{-1}) has decreased and substrate diffusion is no longer rate-limiting (eq 10). In addition, the K_i determined from the hyperbolic inhibition model ($K_i = 0.7 \pm 0.3\ \mu$M) is within experimental error to the K_D determined by the KIE experiments ($K_D = 0.6 \pm 0.2\ \mu$M), indicating that the inhibition and the increase in KIE are both due to OS binding.

These three independent experimental results (increase in the KIE, hyperbolic inhibition, and loss of the viscosity dependence) all indicate a decrease in commitment and are best explained by the presence of an allosteric site. The lowered commitment (k_2/k_{-1}) is possibly achieved by an OS-induced conformational change in SLO-1 which lowers the affinity for substrate by a factor of 4.6 [i.e., k_{-1} (off-rate) increases, $\alpha = 4.6 \pm 0.5$] and lessens the rate of catalysis by 15% (i.e., k_2 decreases, $\beta = 0.85$). It is clear that the increased off-rate (k_{-1}) is the dominant factor in the kinetic rate change and hence has the more pronounced effect on the enzymatic inhibition (Figures 4−6). This inhibitor-based conformational change is supported by trypsin digest studies of SLO-1 which reveal differences in proteolysis patterns upon binding of OA (*25*, *26*). It should be noted that our model cannot distinguish between two molecules binding within the catalytic site (i.e., one OS and one LA) or OS binding to a completely separate binding site. We are currently performing further studies to locate the allosteric site and characterize the molecular determinants of OS binding.

15-HLO also displays kinetic properties consistent with the presence of an allosteric site. The KIE increases with addition of OS (K_D of $0.4 \pm 0.05\ \mu$M), and the steady-state kinetics (k_{cat}/K_m) saturate at ≈16 μM OS, both indicative of a decrease in commitment, as seen for SLO-1 in this paper. Although α and β cannot be determined due to FA aggregation, the qualitative hyperbolic response of the KIE and the k_{cat}/K_m for 15-HLO upon addition of OS strongly suggests the presence of an allosteric site. Further studies are currently in progress to fully characterize this allosteric site in 15-HLO and determine its inhibition parameters (i.e., α and β).

In conclusion, the current data indicate that OS is a potent lipoxygenase inhibitor that tightly binds to an allosteric site for both SLO-1 and 15-HLO ($K_D = 0.6 \pm 0.2$ and $K_D = 0.45 \pm 0.05$, respectively). The sulfate moiety of OS increases the affinity ≈60-fold over that of the corresponding carboxylic acid in OA for SLO-1 and contributes to the selectivity of OS binding to the allosteric site (OS, $K_D = 0.6\ \mu$M; OA, $K_D \approx 36\ \mu$M; LA, $K_D > 30\ \mu$M). This is significant regarding the inhibition of lipoxygenase since it indicates the allosteric site may be a new chemical target against asthma, atherosclerosis, and cancer.

ACKNOWLEDGMENT

Thanks are given to Dr. M. Knapp and Prof. J. Klinman for helpful discussions and to E. Guenther for technical support. We also thank Prof. D. Deamer for the use of the Cahn electro-microbalance.

REFERENCES

1. Samuelsson, B., Dahlen, S. E., Lindgren, J. A., Rouzer, C. A., and Serhan, C. N. (1987) *Science 237*, 1171−1176.
2. Sigal, E. (1991) *J. Am. Phys. Soc. 260*, 13−28.
3. Gosh, J., and Myers, C. E. (1998) *Proc. Natl. Acad. Sci. U.S.A. 95*, 13182−13187.
4. Nie, D., Hillman, G. G., Geddes, T., Tang, K., Pierson, C., Grignon, D. J., and Honn, K. V. (1998) *Cancer Res. 58*, 4047−4051.
5. Steele, V. E., Holmes, C. A., Hawk, E. T., Kopelovich, L., Lubet, R. A., Crowell, J. A., Sigman, C. C., and Kelloff, G. J. (1999) *Cancer Epidemmiol. Biomarkers Prev. 8*, 467−483.
6. DeGroot, J. J. M. C., Aasa, R., Malmstrom, B. G., Slappendel, S., Veldink, G. A., and Vliegenthart, J. F. G. (1975) *Biochim. Biophys. Acta 377*, 71−79.
7. Gardner, H. W. (1989) *Biochim. Biophys. Acta 1001*, 274−281.
8. Solomon, E. I., Zhou, J., Neese, F., and Pavel, E. G. (1997) *Chem. Biol. 4*, 795−808.
9. Glickman, M. H., and Klinman, J. P. (1996) *Biochemistry 35*, 12882−12892.
10. Glickman, M. H., Wiseman, J. S., and Klinman, J. P. (1994) *J. Am. Chem. Soc. 116*, 793−794.
11. Glickman, M. H., and Klinman, J. P. (1995) *Biochemistry 34*, 14077−14092.
12. Hwang, C. C., and Grissom, C. B. (1994) *J. Am. Chem. Soc. 116*, 795−796.
13. Lewis, E. R., Johansen, E., and Holman, T. R. (1999) *J. Am. Chem. Soc. 121*, 1395−1396.
14. Wang, Z. X., Killilea, S. D., and Srivastava, D. K. (1993) *Biochemistry 32*, 1500−1509.
15. Sailer, E. R., Schweizer, S., Boden, S. E., Ammon, H. P. T., and Safayhi, H. (1998) *Eur. J. Biochem. 256*, 364−368.
16. Holman, T. R., Zhou, J., and Solomon, E. I. (1998) *J. Am. Chem. Soc. 120*, 12564−12572.
17. Bild, G. S., Ramadoss, C. S., and Axelrod, B. (1977) *Lipids 12*, 732−735.
18. Harkins, W. D., and Anderson, T. F. (1937) *J. Am. Chem. Soc. 59*, 2189−2197.
19. Verhagen, J., Vliegenthart, J. F. G., and Boldingh, J. (1978) *Chem. Phys. Lipids 22*, 255−259.
20. Melander, L., and Saunders, W. H. (1987) *Reaction Rates of Isotopic Molecules*, R. E. Krieger Publishing, FL.
21. Hargreaves, W. R., and Deamer, D. W. (1978) *Biochemistry 17*, 3759−3768.
22. Vanderheijdt, L. M., Feiters, M. C., Navartnam, S., Nolting, H. F., Hermes, C., Veldink, G. A., and Vliegenthart, J. F. G. (1992) *Eur. J. Biochem. 207*, 793−802.
23. Segel, I. H. (1975) *Enzyme Kinetics*, John Wiley and Sons, Inc., New York.
24. Brouwer, A. C., and Kirsch, J. F. (1982) *Biochemistry 21*, 1302−1307.
25. Ramachandran, S., Carroll, R. T., Dunham, W. R., and Funk, M. O. (1992) *Biochemistry 31*, 7700−7706.
26. Ramachandran, S., Richardssucheck, T. J., Skrzypczakjankun, E., Wheelock, M. J., and Funk, M. O. (1995) *Biochemistry 34*, 14868−14873.

BI992805T